

A SHELL ELEMENT FORMULATION FOR THE SIMULATION OF PROPAGATING DELAMINATION AND THROUGH-THICKNESS CRACKS

J. Brouzoulis¹, M. Fagerström^{*1}, E. Svenning¹

¹Department of Applied Mechanics, Chalmers University of Technology, Gothenburg, Sweden

* Corresponding Author: martin.fagerstrom@chalmers.se

Keywords: multiple delaminations, through-thickness cracks, shell elements, XFEM,

Abstract

In this contribution, we propose an enhanced shell element formulation for mesh independent FE simulation of through-thickness and multiple delamination crack propagation in orthotropic laminates, cf. Figure 1 for an illustration of the possibilities of using this shell element (multiple delaminations). The ambition is to offer a finite element tool to be used for larger component simulations, without having to resort to explicit resolution of each laminae in the laminated structure by three dimensional solid elements or stacked shell elements. The formulation involves three different types of displacement enrichments to make sure that each delaminated subsection which is also cut by a through thickness crack can be individually represented without (unphysical) kinematical couplings to the surrounding structure in the laminate. So far, the proposed modelling framework has been validated against pure deformation modes, in terms of either multiple delaminations or a through-thickness crack.

1. Introduction

The ability to investigate the crashworthiness of fibre reinforced vehicle structures, by efficient numerical simulations, is crucial for FRP lightweight materials to see widespread use in future cars. Consequently, for an accurate prediction of the crashworthiness performance, careful considerations of the underlying failure mechanisms are necessary for the proper modelling of progressive laminate failure in this type of application. However, in addition to the relevance and accuracy of the adopted material model, also the computational efficiency of the structural analysis is essential. This, in order to enable full car crash Finite Element (FE) analyses, meeting today's development lead times in the automotive industry.

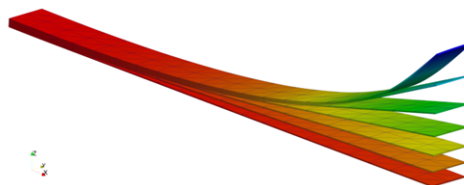


Figure 1. Results obtained by modelling multiple delaminations within the same shell using the formulation proposed in Reference [1], cf. also the first numerical example below.

One approach to meet the requirements of computational efficiency would be to restrict the finite element analysis to shells only, and to only allow one shell element through the thickness. This, however, poses at least two requirements on the shell formulation itself: *i*) the stress variation through the laminate is accurately captured and *ii*) the shell kinematics allows also for the modelling of failure mechanisms such as delaminations and cracks. In a parallel contribution, the first requirement is addressed using a multiscale approach where the laminate is locally resolved by a 3D representative volume element, cf. Främby *et al.* for details [2]. In the current contribution we instead focus on the second challenge, thereby proposing an enhanced shell element formulation based on the eXtended Finite Element Method (XFEM) for mesh independent FE simulation of through-thickness and delamination crack propagation in orthotropic laminates. Consequently, kinematical enrichments are added to the basic shell representation in order to describe delamination cracks and through-thickness cracks. The proposed formulation herein is an extension of the recently proposed shell element for the analysis of multiple delaminations [1], cf. Figure 1 for an illustration of the possibilities of using this formulation, formulated along the lines set out in Larsson *et al.* [3]. In this context, we acknowledge the previous developments using XFEM to model failure in composites, *e.g.* de Borst and Remmers [4] modelling arbitrary delaminations and Van der Meer *et al.* [5] modelling matrix cracks and delaminations by XFEM enhanced solid elements (matrix cracks) and interconnecting classical cohesive elements (delaminations).

As a consequence of the adopted kinematics with local enrichments, propagation of both delamination and through-thickness cracks can be treated simultaneously and independently of the spatial discretisation, thereby reducing the computational effort required in large scale analyses. It is emphasised that the level of detail in the present approach is such that individual delaminations can be analysed using a mixed mode cohesive zone approach; however, it is not fine enough to capture cracks growing through individual laminae. The latter are instead to be incorporated in a 'smeared' sense by a material model including damage in the spirit of Maimí *et al.* [6] which incorporates the relevant failure mechanisms. Thus, focus is on the representation of 'global' cracking of the laminate where discrete cracks can be incorporated when the structural integrity is lost or nearly lost. So far, the kinematical implementation has been verified, as shown in the numerical examples of this paper.

2. Continuous shell kinematics

To set the stage, we first briefly describe the underlying shell kinematics for a non-delaminated shell, which in the subsequent section then will be extended to allow for arbitrarily many delaminations as well as a through thickness crack.

2.1. Initial shell geometry and convected coordinates

As a starting point, the initial configuration B_0 of the shell is considered parameterised in terms of convected (covariant) coordinates (ξ_1, ξ_2, ξ) as

$$B_0 = \left\{ \mathbf{X} := \mathbf{\Phi}(\boldsymbol{\xi}) = \bar{\mathbf{\Phi}}(\bar{\boldsymbol{\xi}}) + \xi \mathbf{M}(\bar{\boldsymbol{\xi}}) \right. \\ \left. \text{with } (\bar{\boldsymbol{\xi}}) \in A \text{ and } \xi \in \frac{h_0}{2} [-1, 1] \right\} \quad (1)$$

where we introduced the contracted notation $\boldsymbol{\xi} = (\xi_1, \xi_2, \xi)$ and $\bar{\boldsymbol{\xi}} = (\xi_1, \xi_2)$ and where the mapping $\mathbf{\Phi}(\boldsymbol{\xi})$ maps the inertial Cartesian frame into the undeformed configuration, cf. Figure 2. In

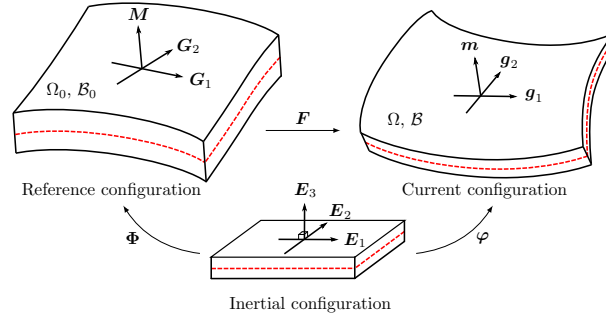


Figure 2. Mappings of shell model defining undeformed and deformed shell configurations relative to inertial Cartesian frame.

Eq (1), the mapping Φ is defined by the midsurface placement $\bar{\Phi}$ and the outward unit normal vector field \mathbf{M} (with $|\mathbf{M}| = 1$). The coordinate ξ is associated with this direction and h_0 is the initial thickness of the shell.

Furthermore, it should be noted that

$$\begin{aligned} d\mathbf{X} &= (\mathbf{G}_\alpha \otimes \mathbf{G}^\alpha) \cdot d\mathbf{X} + \mathbf{M} \otimes \mathbf{M} \cdot d\mathbf{X} = \\ &= \mathbf{G}_\alpha(\xi) d\xi_\alpha + \mathbf{M}(\xi) d\xi \end{aligned} \quad (2)$$

whereby the co-variant basis vectors are defined by

$$\mathbf{G}_\alpha = \bar{\Phi}_{,\alpha} + \xi \mathbf{M}_{,\alpha} \quad \alpha = 1, 2 \quad (3)$$

$$\mathbf{G}_3 = \mathbf{G}^3 = \mathbf{M} \quad (4)$$

where $\bullet_{,\alpha}$ denotes the derivative with respect to ξ_α .

2.2. Current shell geometry

The current (deformed) geometry is in the present formulation described by the deformation map $\varphi(\xi) \in \mathcal{B}$ of the inertial Cartesian frame as

$$\mathbf{x}(\xi) = \bar{\varphi}(\bar{\xi}) + \xi \mathbf{m}(\bar{\xi}) + \frac{1}{2} \xi^2 \gamma(\bar{\xi}) \mathbf{m}(\bar{\xi}) \quad (5)$$

where the mapping is defined by the midsurface placement $\bar{\varphi}$, the spatial director field \mathbf{m} and an additional scalar thickness inhomogeneity strain γ , cf. also Figure 2. As can be seen, the specification of the current configuration corresponds to a second order Taylor expansion along the director field, involving the inhomogeneity strain γ , thereby describing inhomogeneous thickness deformation effects of the shell. In particular, the pathological Poisson locking effect is avoided in this fashion. To identify the corresponding deformation gradient, a relative motion $d\mathbf{x}$ of the non-linear placement φ is considered as

$$d\mathbf{x} = \left(\bar{\varphi}_{,\alpha} + \mathbf{m}_{,\alpha} \left(\xi + \frac{1}{2} \gamma \xi^2 \right) + \frac{1}{2} \gamma_{,\alpha} \xi^2 \mathbf{m} \right) d\xi_\alpha + \mathbf{m} (1 + \gamma \xi) d\xi \quad (6)$$

whereby the deformation gradient \mathbf{F} is defined as

$$d\mathbf{x} = \mathbf{F} \cdot d\mathbf{X} \quad \text{with } \mathbf{F} = \mathbf{g}_i \otimes \mathbf{G}^i, \quad i = 1, 2, 3 \quad (7)$$

In Eq. (7), the spatial co-variant basis vectors are identified from Eq. (6) as

$$\mathbf{g}_\alpha = \bar{\varphi}_{,\alpha} + \left(\xi + \frac{1}{2} \gamma \xi^2 \right) \mathbf{m}_{,\alpha} + \frac{1}{2} \gamma_{,\alpha} \xi^2 \mathbf{m} \quad \alpha = 1, 2, \quad \mathbf{g}_3 = (1 + \gamma \xi) \mathbf{m} \quad (8)$$

3. Discontinuity enhanced kinematics

As stated above, the primary focus of the current work is to develop a shell element formulation able to represent arbitrarily many delaminations in combination with also a through the thickness crack within one and the same element. Consequently, the above basic shell kinematics need to be extended to allow for displacement and director discontinuities across each delamination interface $\Gamma_{S_k^D}$ and across the through thickness crack interface Γ_{S^C} . For this purpose, we propose herein a kinematical extension in line with the XFEM (or partition of unity concept) such that the deformation map into the spatial deformed configuration is subdivided into one continuous and one discontinuous part as

$$\mathbf{x}(\xi) = \boldsymbol{\varphi}^c(\xi) + \boldsymbol{\varphi}^d(\xi) \quad (9)$$

where the continuous part takes on the same form as the underlying non-delaminated shell element.

$$\boldsymbol{\varphi}^c(\xi) = \bar{\boldsymbol{\varphi}}^c(\bar{\xi}) + \xi \mathbf{m}^c(\bar{\xi}) + \frac{1}{2} \xi^2 \gamma(\bar{\xi}) \mathbf{m}^c(\bar{\xi}) \quad (10)$$

As for the discontinuous part $\boldsymbol{\varphi}^d$, it is considered to consist of at most three parts; $\boldsymbol{\varphi}^D$ representing all the possible delaminations, $\boldsymbol{\varphi}^C$ representing the through thickness crack discontinuity and $\boldsymbol{\varphi}^{DC}$ which – where applicable – takes into consideration the interaction between delaminations and the through thickness crack. As a consequence, we have

$$\boldsymbol{\varphi}^d = \boldsymbol{\varphi}^D + \boldsymbol{\varphi}^C + \boldsymbol{\varphi}^{CD} \quad (11)$$

with:

$$\boldsymbol{\varphi}^D = \sum_{k=1}^{N_{\text{del}}} \mathcal{H}_S(S_k^D(\mathbf{X})) (\bar{\boldsymbol{\varphi}}^{Dk}(\bar{\xi}) + \xi \mathbf{m}^{Dk}(\bar{\xi})) = \mathcal{H}_{S_k^D}^D (\bar{\boldsymbol{\varphi}}^{Dk} + \xi \mathbf{m}^{Dk}) \quad (\text{sum over } k) \quad (12)$$

$$\boldsymbol{\varphi}^C = \sum_{I \in N_{\text{enr}}} N^I[\xi_1, \xi_2] \psi^I[\xi_1, \xi_2] (\bar{\boldsymbol{\varphi}}_C^I + \xi \mathbf{m}_C^I) \quad (13)$$

$$\boldsymbol{\varphi}^{CD} = \sum_{k=1}^{N_{\text{del}}} \sum_{I \in N_{\text{enr}}} \mathcal{H}_S(S_k^D(\mathbf{X})) N^I[\xi_1, \xi_2] \psi^I[\xi_1, \xi_2] (\bar{\boldsymbol{\varphi}}_{CDk}^I + \xi \mathbf{m}_{CDk}^I) \quad (14)$$

It should be noted that the pure delamination enrichment in Eq. (12) follow the approach proposed in Reference [1], consisting of a sum of enrichments – one for each delamination N_{del} – according to the XFEM concept, however restricted only to discontinuous enrichment of the midsurface placement and the director field. Here, $\mathcal{H}_S(S_k^D(\mathbf{X})) = \mathcal{H}_{S_k^D}^D$ is introduced as the standard Heaviside function pertaining to the particular delamination surface $\Gamma_{S_k^D}$ where S_k^D is an associated level set function defining the position $\bar{\xi}_k$ (in thickness direction) of this surface. In particular, S_k^D is the signed distance function to the delamination interface k such that, for the current approach where we restrict the initial director field to coincide with the outward normal vector, it can be defined simply as

$$S_k^D = \xi - \bar{\xi}_k \quad \text{whereby} \quad \frac{\partial S_k^D}{\partial \mathbf{X}} = \mathbf{M} \quad (15)$$

where \mathbf{M} is the normal to each delamination surface in the reference configuration. Furthermore, $\bar{\boldsymbol{\varphi}}^{Dk}$ and \mathbf{m}^{Dk} are approximated in a normal fashion using standard quadratic shape functions.

In addition to this, we add the enrichment to describe a through-thickness crack $\boldsymbol{\varphi}^C$ in the case of no delaminations. Here, we follow the procedure proposed initially by Larsson *et al.* [3] further extended in Mostofizadeh *et al.* [7]. Thus, the 'shifted' form of the Heaviside function ψ^I is utilised to realise the strong discontinuity. Hence, in analogy with *e.g.* Zi and Belytschko [8], we let N_{enr} denote the set of enriched nodes to describe the through-thickness crack and we have the shifted enrichment function (associated with such each node I) defined as

$$\psi^I[\xi_1, \xi_2] = \mathcal{H}_S[S^C[\xi_1, \xi_2]] - \mathcal{H}_S[S^C[\xi_1^I, \xi_2^I]] \quad (16)$$

where in this case S^C is a different level set function (in-plane in contrast to S_k^D which is defined out of the shell plane) and where $\bar{\boldsymbol{\varphi}}_C^I$ and \mathbf{m}_C^I are the degrees-of-freedom representing the discontinuous parts of the midsurface displacement and director field respectively. More precisely, the argument of the Heaviside function, the level-set function $S^C[\xi_1, \xi_2]$ defined on D_0 , is considered monotonic so that

$$\begin{cases} S[\xi_1, \xi_2] < 0 & \text{if } \boldsymbol{\Phi}[\xi_1, \xi_2] \in D_0^- \\ S[\xi_1, \xi_2] = 0 & \text{if } \boldsymbol{\Phi}[\xi_1, \xi_2] \in \Gamma_S \\ S[\xi_1, \xi_2] > 0 & \text{if } \boldsymbol{\Phi}[\xi_1, \xi_2] \in D_0^+ \end{cases} \quad (17)$$

where D_0 is the local enrichment domain in the vicinity of the crack. It is remarked that the enriched reference domain D_0 is here defined only by the finite elements intersected by a through-thickness crack (or possibly a cohesive segment) since the enrichment functions in Eq. (16) are defined so that the discontinuous enrichment vanishes at the (corner) nodes. D_0 is considered subdivided into a minus side D_0^- and a plus side D_0^+ by the discontinuity line Γ_{Sc} with corresponding normal vector \mathbf{N}_{Sc} . Please note that the level-set function S^C has the convected midsurface coordinates as arguments, thereby restricting the current formulation to through-the-thickness shell fracture.

The above two enrichments $\boldsymbol{\varphi}^D$ and $\boldsymbol{\varphi}^C$ are sufficient to obtain a formulation that can handle *either* multiple delaminations or a through thickness crack in one and the same element. However, since we are after a formulation which is also able to treat the combined case where multiple delaminations and a through thickness crack can coexist, yet another enrichment $\boldsymbol{\varphi}^{CD}$ as given in Eq. (14) is required. This is in analogy to the case of at least two intersecting through-thickness cracks, as described by Daux *et al.* [9]. In essence, the additional enrichment function is a product between the ones for the delaminations and the one for the through-thickness crack.

The procedure for establishing the shell element formulation based on these kinematics follows exactly Reference [1], *i.e.* first the deformation gradient \mathbf{F} is established based on the extended kinematics which takes the general form:

$$\mathbf{F} = \left(\boldsymbol{\varphi}^c(\boldsymbol{\xi}) + \boldsymbol{\varphi}^D(\boldsymbol{\xi}) + \boldsymbol{\varphi}^C(\boldsymbol{\xi}) + \boldsymbol{\varphi}^{CD}(\boldsymbol{\xi}) \right) \otimes \nabla_{\mathbf{X}} = \mathbf{F}^b + \delta_{S^D} \mathbf{F}_k^D + \delta_{S^C} \mathbf{F}^C \quad (\text{sum over } k) \quad (18)$$

where

$$\mathbf{F}^b = \mathbf{g}_j^b \otimes \mathbf{G}^j, \quad j = 1, 2, 3 \quad (19)$$

and where \mathbf{g}_j^b are the spatial co-variant basis vectors and

$$\mathbf{F}_k^D = \left(\bar{\varphi}^{Dk} + \xi \mathbf{m}^{Dk} + \bar{\varphi}^{CDk} + \xi \mathbf{m}^{CDk} \right) \otimes \mathbf{M} \quad (20)$$

$$\mathbf{F}_k^C = \left(\bar{\varphi}^C + \xi \mathbf{m}^C + \sum_{k=1}^{N_{del}} \sum_{I \in N_{enr}} \mathcal{H}_{S_k}^D N^I [\xi_1, \xi_2] \left(\bar{\varphi}_{CDk}^I + \xi \mathbf{m}_{CDk}^I \right) \right) \otimes N_{Sc} \quad (21)$$

Please note that $\delta_{S_k^D}$ and δ_{S^C} refers to Dirac delta functions defined with respect to each respective discontinuity (crack) surface and that:

$$\bar{\varphi}^{CDk} = \sum_{I \in N_{enr}} N^I \psi^I \bar{\varphi}_{CDk}^I, \quad \mathbf{m}^{CDk} = \sum_{I \in N_{enr}} N^I \psi^I \mathbf{m}_{CDk}^I, \quad \bar{\varphi}^C = \sum_{I \in N_{enr}} N^I \bar{\varphi}_C^I, \quad \mathbf{m}^C = \sum_{I \in N_{enr}} N^I \mathbf{m}_C^I \quad (22)$$

This is then inserted in the classical momentum balance, yielding the stress resultant shell formulation including interface parts where the (continuous) traction is integrated over each delamination surface as well as over the through-thickness crack surface.

4. Numerical examples for validation of the model

To verify the proposed kinematics, two numerical examples are presented. The first example concerns multiple delaminations of a cantilever beam. The second example verifies the capability of the element to represent a crack through the laminate thickness. In the examples, a transversely isotropic elastic material model has been used with material parameters according to Table 1. Furthermore, all laminae have a zero degree orientation.

E_L	126 GPa
$E_T = E_{TT'}$	10 GPa
$G_{LT} = G_{TT'}$	8 GPa
$\nu_{LT} = \nu_{TT'}$	0.29

Table 1. Material parameters used for the numerical examples.

4.1. Cantilever beam with multiple delaminations

The problem consists of a cantilever beam, composed of seven laminae, which has six active delaminations. The length of each crack varies and is given through the parameter $a = 30$ mm, cf. Figure 3 for details. The length of the beam is $L = 200$ mm, has a height of $h = 3$ mm and a width of $w = 15$ mm. The beam is subjected to a constant edge load t at the top of the beam (at its free end) with the magnitude 10 N/m in the vertical direction.

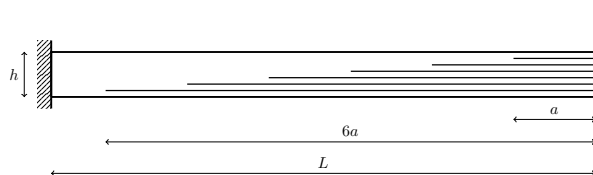


Figure 3. Geometry of the beam with multiple (6) delaminations with different lengths.

In Figure 1, the deformation pattern of the beam has already been shown illustrating that the element can handle multiple delaminations and a comparison with beam theory is shown in

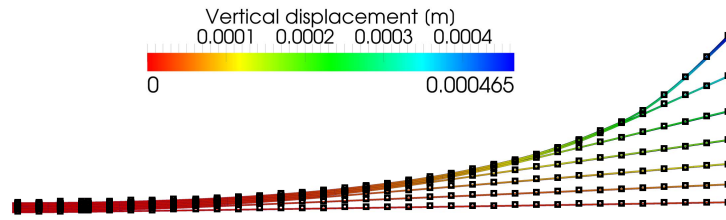


Figure 4. Comparison of FE solution with beam theory where the shell results are overlaid by the analytical results (squares) based on Euler - Bernoulli theory.

Figure 4. It can be seen that the obtained solution corresponds well with beam theory, thus verifying the kinematics of the element. The error in maximum displacement is less than 0.5 % between the two and it is clear that also the other laminae follow the analytical solution.

4.2. Cantilever beam with through the thickness crack

The second example illustrates the capability of the proposed element to handle a crack through the thickness thus cutting the element in two. The studied problem is a cantilever beam of the same geometry as in the previous example; however, in this case only with two 0° laminae. In this case, there are no delaminations. Instead, there is one crack that runs along the whole length of the beam cutting it into two cantilever beams, see Figure 5. The crack is placed at a distance of $b = 6$ mm from the edge thus defining the width of the smaller beam. The beam is subjected to a prescribed vertical displacement in the corner of the beam. Euler-Bernoulli

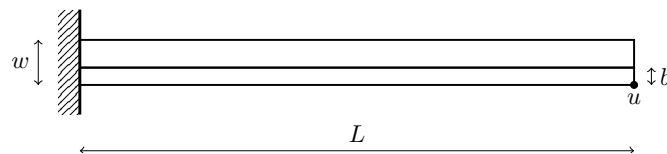


Figure 5. Geometry of the cantilever beam, seen from above, with a through the thickness crack along its entire length.

beam theory gives that the reaction force necessary to vertically move the free edge a distance of $p = 1$ mm is 0.6379 N. The corresponding value obtained from simulation is 0.6384 N which gives a relative error of 0.03%. This verifies that the shell element is capable of accurately representing a through the thickness crack. In Figure 6, the displacement field of the beam is shown and it is clear that it is cut into two pieces. Note also that the sub-triangulation of the elements (those cut by a crack) is shown.

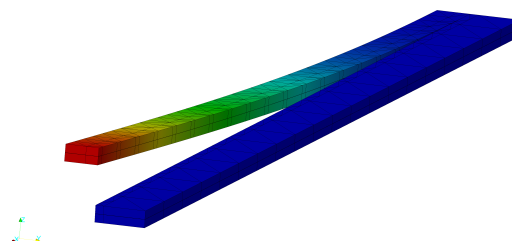


Figure 6. Displacement field for the cantilever beam with a through the thickness crack (magnification factor = 10).

5. Conclusions

A XFEM based shell element formulation has been proposed in this contribution. The kinematical representation is capable of handling multiple delaminations and a through-thickness crack present at the same location in the laminate. The formulation involves three different types of displacement enrichments to make sure that each delaminated subsection which is also cut by a through thickness crack can be individually represented without (unphysical) kinematical couplings to the surrounding structure in the laminate. In this contribution, the proposed modelling framework has been validated against pure deformation modes, in terms of either multiple delaminations or a through-thickness crack. The framework is however more general whereby the next step will be to identify and perform similar validations also for a combined case.

Acknowledgement

The research leading to these results receives funding from the European Communitys Seventh Framework Programme (FP7/2007-2013) under grant agreement no. 314182 (the MATISSE project). This publication solely reflects the authors views. The European Community is not liable for any use that may be made of the information contained herein.

References

- [1] J. Brouzoulis and M. Fagerström. Modelling of multiple delaminations in shells using XFEM. In *Proc. 19th Int. Conf. Composite Materials*. 2013.
- [2] J. Främby, J. Brouzoulis, M. Fagerström, and R. Larsson. A fully coupled multiscale shell formulation for the modelling of fibre reinforced laminates. In *Proc. 16th Eur. Conf. Composite Materials*. 2014.
- [3] R. Larsson, J. Mediavilla, and M. Fagerström. Dynamic fracture modeling in shell structures based on XFEM. *Int. J. Numer. Meth. Eng.*, 86:499–527, 2010.
- [4] R. de Borst and J. Remmers. Computational modelling of delamination. *Compos. Sci. Technol.*, 66:713–722, 2006.
- [5] F.P. van der Meer, L.J. Sluys, S.R. Hallett, and M.R. Wisnom. Computational modeling of complex failure mechanisms in laminates. *J. Compos. Mater.*, 46:603–623, 2011.
- [6] P. Maimí, P.P. Camanho, J.A. Mayugo, and C.G. Dávila. A continuum damage model for composite laminates: Part I - Constitutive model. *Mech. Mater.*, 39:897–908, 2007.
- [7] S. Mostofizadeh, M Fagerström, and R. Larsson. Dynamic crack propagation in elastoplastic thinwalled structures: Modelling and validation. *Int. J. Numer. Meth. Eng.*, 96(2):63–86, 2012.
- [8] G. Zi and T. Belytschko. New crack-tip elements for XFEM and applications to cohesive cracks. *Int. J. Numer. Meth. Eng.*, 57:2221–2240, 2003.
- [9] C. Daux, N. Moës, J. Dolbow, N. Sukumar, and T. Belytschko. Arbitrary branched and intersecting cracks with the extended finite element method. *Int. J. Numer. Meth. Eng.*, 48:1741–1760, 2000.